

## Stability of Cyclic $\beta$ -Hairpins: Asymmetric Contributions from Side Chains of a Hydrogen-Bonded Cross-Strand Residue Pair

Stephen J. Russell, Tamas Blandl, Nicholas J. Skelton, and Andrea G. Cochran\*

*Contribution from the Department of Protein Engineering, Genentech, Inc.,  
1 DNA Way, South San Francisco, California 94080*

Received August 9, 2002; E-mail: andrea@gene.com

**Abstract:** Amino acid structural propensities measured in “host–guest” model studies are often used in protein structure prediction or to choose appropriate residues in de novo protein design. While this concept has proven useful for helical structures, it is more difficult to apply successfully to  $\beta$ -sheets. We have developed a cyclic  $\beta$ -hairpin scaffold as a host for measurement of individual residue contributions to hairpin structural stability. Previously, we have characterized substitutions in non-backbone-hydrogen-bonded strand sites; relative stability differences measured in the cyclic host are highly predictive of changes in folding free energy for linear  $\beta$ -hairpin peptides. Here, we examine the hydrogen-bonded strand positions of our host. Surprisingly, we find a large favorable contribution to stability from a valine (or isoleucine) substitution immediately preceding the C-terminal cysteine of the host peptide, but not at the cross-strand position of the host or in either strand of a folded linear  $\beta$ -hairpin (trpzip peptide). Further substitutions in the peptides and NMR structural analysis indicate that the stabilizing effect of valine is general for CX<sub>8</sub>C cyclic hairpins and cannot be explained by particular side-chain–side-chain interactions. Instead, a localized decrease in twist of the peptide backbone on the N-terminal side of the cysteine allows the valine side chain to adopt a unique conformation that decreases the solvent accessibility of the peptide backbone. The conformation differs from the highly twisted (coiled) conformation of the trpzip hairpins and is more typical of conformations present in multistranded  $\beta$ -sheets. This unexpected structural fine-tuning may explain why cyclic hairpins selected from phage-displayed libraries often have valine in the same position, preceding the C-terminal cysteine. It also emphasizes the diversity of structures accessible to  $\beta$ -strands and the importance of considering not only “ $\beta$ -propensity”, but also hydrogen-bonding pattern and strand twist, when designing  $\beta$  structures. Finally, we observe correlated, cooperative stabilization from side-chain substitutions on opposite faces of the hairpin. This suggests that cooperative folding in  $\beta$ -hairpins and other small  $\beta$ -structures is driven by cooperative strand–strand association.

### Introduction

Much recent work has begun to define the structural features important for stabilization of the  $\beta$ -structure in proteins and peptides.<sup>1</sup> The  $\beta$ -hairpin is an especially popular small model system. In contrast to an isolated  $\alpha$ -helix, the  $\beta$ -hairpin is structurally rather diverse. Turns of different lengths and geometries are observed, sometimes in equilibrium within a single sequence.<sup>1</sup> Strand residues are differentiated by the hairpin hydrogen-bonding pattern: alternate residues participate in cross-strand backbone hydrogen bonds, while the others are oriented with backbone hydrogen bond donors and acceptors facing outward. Hydrogen-bonding strand pairs may also differ from non-hydrogen-bonding pairs in the relative orientation of the  $\alpha$ – $\beta$  bond vectors and in the cross-strand distance between  $\beta$  carbons. These differences, and the right-handed twist present

in  $\beta$  structures, cause one face of the hairpin to be rather open (that where the side chains of non-hydrogen-bonding residues are directed), while the other is sterically less open. Additional aspects of hairpin structure receiving recent attention are differences in strand length and in the positioning of particular cross-strand residue pairs with respect to the  $\beta$ -turn.<sup>2</sup> Because of the complexity of the  $\beta$  structure, the rules governing  $\beta$ -hairpin design are as yet incompletely defined.

We have established a disulfide-cyclized 10-residue hairpin (bhp series) as a simple model system for the study of individual residue contributions to stability.<sup>3</sup> The disulfide can be used as a quantitative probe for folding by monitoring the equilibrium between dithiol and disulfide.<sup>4</sup> This is measured conveniently as an effective concentration ( $C_{\text{eff}}$ ) of the peptide thiols relative to a reference thiol (e.g., glutathione). Differences in the position

(1) (a) Smith, C. K.; Regan, L. *Acc. Chem. Res.* **1997**, *30*, 153–161. (b) Gellman, S. H. *Curr. Opin. Chem. Biol.* **1998**, *2*, 717–725. (c) Ramírez-Alvarado, M.; Kortemme, T.; Blanco, F. J.; Serrano, L. *Bioorg. Med. Chem.* **1999**, *7*, 93–103. (d) Lacroix, E.; Kortemme, T.; Lopez de la Paz, M.; Serrano, L. *Curr. Opin. Struct. Biol.* **1999**, *9*, 487–493. (e) Searle, M. S. *J. Chem. Soc., Perkin Trans. 2* **2001**, 1011–1020.

(2) (a) Stanger, H. E.; Syud, F. A.; Espinosa, J. F.; Giriat, I.; Muir, T.; Gellman, S. H. *Proc. Natl. Acad. Sci. U.S.A.* **2001**, *98*, 12015–12020. (b) Espinosa, J. F.; Muñoz, V.; Gellman, S. H. *J. Mol. Biol.* **2001**, *306*, 397–402. (3) Cochran, A. G.; Tong, R. T.; Starovasnik, M. A.; Park, E. J.; McDowell, R. S.; Theaker, J. E.; Skelton, N. J. *J. Am. Chem. Soc.* **2001**, *123*, 625–632.

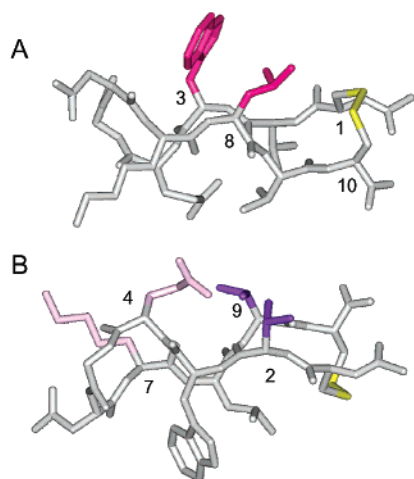


**Figure 1.** Two views of the minimized mean NMR structure of disulfide-cyclized  $\beta$ -hairpin bhpW (1, Chart 1).<sup>3</sup> The cross-strand disulfide between positions 1 and 10 is shown in yellow. (A) Non-hydrogen-bonded (NHB) strand residues are highlighted (Trp3 and Leu8 in magenta). (B) Hydrogen-bonded (HB) strand residues are highlighted (Thr2 and Thr9 in dark purple; Glu4 and Lys7 in lilac).

of the thiol–disulfide equilibrium for different peptides may be compared by calculation of a  $C_{\text{eff}}$  ratio and conversion of the ratio to a free-energy difference ( $\Delta\Delta G_{\text{fold}}$ ).<sup>5</sup> We have found that increases in  $C_{\text{eff}}$  for the bhp peptides correlate with increases in hairpin structure in the oxidized form.<sup>3</sup> In our initial studies, we evaluated the residue preferences at non-hydrogen-bonded (NHB) strand positions 3 and 8 (Figure 1a), finding that tryptophan is by far the most stabilizing residue in either of these positions.<sup>3</sup> More broadly, we found that for a series of hydrophobic substitutions, the residue preferences at the two sites are the same, and that these preferences are largely unchanged by changing the cross-strand partner from leucine to tryptophan.<sup>6</sup> These results suggest that the cross-strand sites are equivalent energetically (despite the fact that they are inequivalent structurally) and that individual residue contributions are the major determinants of hairpin stability, with little or no contribution from specific side-chain–side-chain contacts between cross-strand partners.

Using this information, we replaced the disulfide in our Trp3, Trp8 cyclic hairpins with a second tryptophan–tryptophan pair, obtaining linear 12-residue  $\beta$ -hairpins that fold stably and cooperatively in water (dubbed “tryptophan zippers” or “trpzips”).<sup>7</sup> Interestingly, changes in stability observed upon making residue substitutions in the trpzips NHB strand sites corresponded well with  $\Delta\Delta G$  values measured for substitutions at positions 3 and 8 in the cyclic bhp series. This indicates that residue preferences at these positions are unaffected by the presence of the disulfide, despite observations that disulfides are not ideally suited to span the distance between antiparallel strands,<sup>3,8</sup> and could therefore strain the backbone of the cyclized hairpin.<sup>9</sup>

In the present study, we investigate substitutions at the hydrogen-bonding (HB) strand positions 2 and 9 of the bhp hairpins. We find that the stability determinants at these sites are different from those at the NHB positions 3 and 8. In marked contrast to the observed equivalence of positions 3 and 8, we find that positions 2 and 9 have very different residue preferences from each other. In particular, we find a very large stabilization to the cyclic hairpin fold from a valine residue at position 9; a much smaller stabilization occurs in Val2 variants. This effect is evident from  $C_{\text{eff}}$ -derived free-energy differences and from the NMR structural analysis of Val9 and Val2 bhp analogues. In a trpzips peptide, the HB positions analogous to bhp residues 2 and 9 appear to be energetically equivalent, suggesting that the strong stabilizing effect of Val9 in the bhp peptides is a consequence of its proximity to the cross-strand disulfide. A detailed examination of the bhp peptide NMR structures indicates that the most likely explanation is a localized change in backbone conformation between positions 9 and 10 (relative to the trpzips peptides), rather than the presence of the disulfide per se. Intriguingly, Val9 is often present in disulfide-cyclized  $\beta$ -hairpins selected from phage-displayed peptide libraries, suggesting that its stabilizing effect is general for this fold.

Finally, we analyze the energetic relationship between the 2,9-HB pair and position 3 on the opposite face of the hairpin. Our results show that residue preferences at position 3 are the same in Thr2–Thr9 and His2–Val9 backgrounds. However, the free energies are not strictly additive. Instead, substitution free energies in the two peptide series are linearly correlated with a slope of 2. The larger differences occur in the more stable His2–Val9 hairpin. In previous studies, we observed a similar linear free-energy relationship (with nonunit slope) between positions 3 and 8 but strict additivity between position 3 and the  $\beta$ -turn.<sup>3,6</sup> Taken together, these results demonstrate that for these minimal  $\beta$ -hairpins, strand–strand association is positively cooperative, while the turn and strands contribute independently to stability.

## Experimental Section

**Peptide Synthesis and Purification.** Peptides were synthesized as C-terminal amides using standard Fmoc chemistry on a Pioneer synthesizer (PE Biosystems). Peptides were cleaved from resin by treatment with 5% triisopropyl silane in trifluoroacetic acid (TFA) for 1.5–4 h at room temperature. After TFA was removed by rotary evaporation, peptides were precipitated by addition of ethyl ether and then purified by reversed-phase HPLC (acetonitrile/H<sub>2</sub>O/0.1% TFA). Peptide identity was confirmed by electrospray mass spectrometry. Peptides were converted to cyclic disulfides by dropwise addition of a saturated solution of I<sub>2</sub> in acetic acid to HPLC fractions (until a persistent yellow color was obtained). After lyophilization, the oxidized peptides were repurified by HPLC. Purified peptides eluted as single symmetric peaks on C18 analytical columns (0–40% acetonitrile in 40 min).

**Measurement of Cysteine Effective Concentrations.** Effective concentrations ( $C_{\text{eff}}$ ) were measured relative to the reference thiol glutathione at 20 °C (293 K) as described previously.<sup>3</sup> As before, glutathione stock solutions contained 3 volumes of 0.2 M reduced glutathione (GSH) and 1 volume of 0.1 M oxidized glutathione (GSSG). Thiol–disulfide equilibria were established by mixing 50  $\mu$ L of peptide

(4) (a) Milburn, P. J.; Konishi, Y.; Meinwald, Y. C.; Scheraga, H. A. *J. Am. Chem. Soc.* **1987**, *109*, 4486–4496. (b) Milburn, P. J.; Meinwald, Y. C.; Takahashi, S.; Ooi, T.; Scheraga, H. A. *Int. J. Pept. Protein Res.* **1988**, *31*, 311–321. (c) Falcomer, C. M.; Meinwald, Y. C.; Choudhary, I.; Talluri, S.; Milburn, P. J.; Clardy, J.; Scheraga, H. A. *J. Am. Chem. Soc.* **1992**, *114*, 4036–4042. (d) Stroup, A. N.; Gierasch, L. M. *Biochemistry* **1990**, *29*, 9765–9771.

(5) Lin, Y.-T.; Kim, P. S. *Biochemistry* **1989**, *28*, 5282–5287.

(6) Russell, S. J.; Cochran, A. G. *J. Am. Chem. Soc.* **2000**, *122*, 12600–12601.

(7) Cochran, A. G.; Skelton, N. J.; Starovasnik, M. A. *Proc. Natl. Acad. Sci. U.S.A.* **2001**, *98*, 5578–5583. (Correction: Cochran, A. G.; Skelton, N. J.; Starovasnik, M. A. *Proc. Natl. Acad. Sci. U.S.A.* **2002**, *99*, 9081.)

(8) (a) Gunasekaran, K.; Ramakrishnan, C.; Balam, P. *Protein Eng.* **1997**, *10*, 1131–1141. (b) Hutchinson, E. G.; Sessions, R. B.; Thornton, J. M.; Woolfson, D. N. *Protein Sci.* **1998**, *7*, 2287–2300.

(9) Aberle, A. M.; Reddy, H. K.; Heeb, N. V.; Nambiar, K. P. *Biochem. Biophys. Res. Commun.* **1994**, *200*, 102–107.

stock (approximately 3 mM in water) with 50  $\mu$ L of glutathione stock.  $C_{\text{eff}}$  values were calculated from the molar ratios of the reduced and oxidized forms of peptide and glutathione:

$$C_{\text{eff}} = ([\text{peptide}_{\text{ox}}]/[\text{peptide}_{\text{red}}]) \cdot ([\text{GSH}]^2/[\text{GSSG}])$$

Two or three samples from each reaction mixture were analyzed; there were no shifts in populations with time, and calculated  $C_{\text{eff}}$  values typically varied by less than 5% (equivalent to 30 cal mol<sup>-1</sup> uncertainty in  $\Delta\Delta G$ ).  $C_{\text{eff}}$  values were independent of peptide concentration.

**NMR Data Collection and Analysis.** One- and two-dimensional (2QF-COSY, TOCSY, ROESY, COSY-35) <sup>1</sup>H NMR spectra of each peptide were acquired on a Bruker AMX500 spectrometer at temperatures between 5 and 30 °C in 90% H<sub>2</sub>O/10% D<sub>2</sub>O or 100% D<sub>2</sub>O. Samples contained a 1–5 mM solution of peptide at pH 5.0. Spectra were processed and analyzed with FELIX (Accelrys, San Diego). Resonance assignments were made by standard stepwise spin-system identification and sequential through-space interaction methods.<sup>10</sup> <sup>3</sup>J<sub>HN-H $\alpha$</sub>  were obtained by fitting Lorentzian lines to the antiphase doublets of H<sup>N</sup>–H <sup>$\alpha$</sup>  peaks in 2QF-COSY spectra processed to high digital resolution in  $F_2$ . <sup>3</sup>J<sub>H $\alpha$ -H $\beta$</sub>  were extracted from the COSY-35 spectra collected in D<sub>2</sub>O.

**Structure Calculations.** Interproton distance restraints were generated from ROE peaks observed in ROESY spectra collected in both H<sub>2</sub>O and D<sub>2</sub>O.<sup>11</sup>  $\phi$  and  $\chi_1$  dihedral angle restraints were derived from <sup>3</sup>J<sub>HN-H $\alpha$</sub>  and <sup>3</sup>J<sub>H $\alpha$ -H $\beta$</sub>  scalar coupling constants, respectively.<sup>11</sup> One hundred structures were calculated with the program DGII,<sup>12</sup> using the CVFF force field parameters (Accelrys, San Diego). The 80 structures of lowest DGII penalty function were further refined with the Sander module of AMBER, version 6.0.<sup>13</sup> For comparison purposes, an ensemble was also calculated for bhpW using this protocol (rather than the DISCOVER restrained molecular dynamics refinement reported previously<sup>3</sup>). Each structure was annealed by equilibrating at 0 K for 500 steps (time step = 0.001 ps), heating to 1000 K over 500 steps, maintaining this temperature for 3500 steps, and cooling back to 0 K over 1500 steps. Force constants for the experimental restraints were increased linearly over the first 3000 steps of this protocol to final values of 20 kcal mol<sup>-1</sup> Å<sup>-2</sup> and 50 kcal mol<sup>-1</sup> rad<sup>-2</sup> for distance and dihedral angle restraints, respectively. The structures were then energy minimized for 250 steps with the force constants at full value. A distance-dependent dielectric was used throughout, with partial atomic charges of charged side chains scaled by a factor of 0.2. Restraints were also included to maintain the appropriate geometry of chiral centers (force constant = 10 kcal mol<sup>-1</sup> rad<sup>-2</sup>) and the planarity of peptide bonds (force constant = 50 kcal mol<sup>-1</sup> rad<sup>-2</sup>). Restraints based on <sup>1</sup>H NMR chemical shifts<sup>14</sup> were included both for  $\alpha$ -protons and for protons from side chains determined to reside in a single  $\chi_1$  rotamer well on the basis of <sup>3</sup>J<sub>H $\alpha$ -H $\beta$</sub>  coupling constant values (Table 1). These restraints were enforced with square-well potentials with flat bottoms (observed shift  $\pm$  0.1 ppm) and a force constant of 10 kcal mol<sup>-1</sup> ppm<sup>-2</sup>. In the initial structures calculated for bhpW and VH, two populations were observed for the disulfide bond geometry. The less populated family had  $\chi_1$  values close to  $-90^\circ$ ,  $\chi_2$  values close to  $+40^\circ$ , and  $\chi_3$  values close to  $-100^\circ$ . Because this  $\chi_1$  is not in full agreement with the observed <sup>3</sup>J<sub>H $\alpha$ -H $\beta$</sub>  and the  $\chi_2$  is not favorable,<sup>15</sup> the calculations were repeated with restraints to force the structures to adopt the geometry

**Table 1.** <sup>3</sup>J<sub>H $\alpha$ -H $\beta$</sub>  for Hydrogen-Bonded Cross-Strand Residues

peptide	position 2 <sup>a</sup>		position 9 <sup>a</sup>		$C_{\text{eff}}$ , mM
	<sup>3</sup> J <sub>H<math>\alpha</math>-H<math>\beta</math></sub> , Hz	$\chi_1$	<sup>3</sup> J <sub>H<math>\alpha</math>-H<math>\beta</math></sub> , Hz	$\chi_1$	
bhpW (TT; <b>1</b> )	7.9	n.d. <sup>c</sup>	6.8	n.d.	210
HV; <b>15</b>	<u>3.8, 3.8<sup>b</sup></u>	<u>+60°</u>	<u>9.8</u>	<u>180°</u>	1181
VH; <b>14</b>	5.6	n.d.	7.4, 7.6	n.d.	293
TV; <b>12</b>	4.2	<u>+60°</u>	<u>9.7</u>	<u>180°</u>	677
VT; <b>6</b>	5.9	n.d.	6.5	n.d.	305
trpzp 7 (VH)	7.8	n.d.	6.0, 6.9	n.d.	n.a. <sup>d</sup>
trpzp 8 (HV)	6.2, 6.5	n.d.	7.9	n.d.	n.a.

<sup>a</sup> The equivalent positions are 4 and 13 for trpzips 7 and 8 (see Chart 2). <sup>b</sup> Values representing nonaveraging  $\chi_1$  torsion angles are underlined. <sup>c</sup> Not defined. <sup>d</sup> Not applicable.

observed in the more populous initial family ( $-120^\circ < \chi_2 < -70^\circ$  and  $+80^\circ < \chi_3 < +120^\circ$ ). The latter disulfide bond geometry was observed in the HV structures without additional restraints. The 20 conformations of lowest restraint violation energy had no distance or dihedral angle restraint violations greater than 0.1 Å or 1.0°, respectively, and were chosen to represent the structures. All backbone conformations were in “preferred” or “allowed” regions of  $\phi, \psi$  space, as judged by the program PROCHECK.<sup>16</sup> Details of the input restraints and resulting ensembles are presented in Supporting Information Table 10.

**Measurement of Interstrand Twist.** The twist between residues  $i$  and  $i + 1$  of one strand and residues  $j$  and  $j - 1$  of the opposite strand, designated  $\Theta$ , was measured from the dihedral angle formed by  $C_i^\alpha - (C_i^\alpha \wedge C_j^\alpha) - (C_{i+1}^\alpha \wedge C_{j-1}^\alpha) - C_{i+1}^\alpha$ , where the “(x $\wedge$ y)” indicates the midpoint between atoms  $x$  and  $y$ .<sup>17</sup> The vector  $(C_i^\alpha \wedge C_j^\alpha) - (C_{i+1}^\alpha \wedge C_{j-1}^\alpha)$  approximates the axis of twist, and  $\Theta$  has a positive value for a right-handed twist. This definition of  $\Theta$  differs from published definitions<sup>17,18</sup> in that interstrand twist is calculated at each strand position rather than over two strand positions; therefore, the maximum value of  $\Theta$  expected for antiparallel strands is  $\pm 35^\circ$  instead of  $\pm 70^\circ$ .

**Thermal Denaturation of Trpzp Peptides.** Samples contained 20  $\mu$ M peptide in 20 mM potassium phosphate, pH 7.0. The folded structure was monitored by circular dichroism at 229 nm. Thermal melts were acquired and analyzed as previously described for trpzp4.<sup>7</sup>

## Results

To evaluate the residue preferences at hydrogen-bonded strand positions of  $\beta$ -hairpins, we chose our previously reported cyclic peptide bhpW **1** as a host (Chart 1). This peptide adopts a well-defined hairpin conformation, and we have determined its structure by NMR (Figure 1).<sup>3</sup> The disulfide of bhpW helps to stabilize the hairpin conformation and simultaneously provides an assay for structure. Changes in hairpin stability can be quantified by changes in the position of the thiol–disulfide equilibrium.<sup>3</sup> Residues 2 and 9 of bhpW are cross-strand from one another and form backbone hydrogen bonds. We therefore introduced several substitutions at positions 2 and 9 in bhpW (Chart 1).

The relative stabilities of the bhpW variants were determined from the effective concentrations ( $C_{\text{eff}}$ ) of the cysteine thiols (see Experimental Section and Supporting Information) and are shown in Figure 2. Substitutions at both positions have large effects on hairpin stability. The range of stabilities is 1 kcal mol<sup>-1</sup> for substitutions at position 2 (Figure 2b) and 0.7 kcal mol<sup>-1</sup> for the same substitutions at position 9 (Figure 2c). The

(10) Wüthrich, K. *NMR of Proteins and Nucleic Acids*; John Wiley and Sons: New York, 1986.

(11) Skelton, N. J.; Garcia, K. C.; Goeddel, D. V.; Quan, C.; Burnier, J. P. *Biochemistry* **1994**, *33*, 13581–13592.

(12) Havel, T. F. *Prog. Biophys. Mol. Biol.* **1991**, *56*, 43–78.

(13) (a) Weiner, S. J.; Kollman, P. A.; Case, D. A.; Singh, U. C.; Ghio, C.; Alagona, G.; Profeta, J. S.; Weiner, P. *J. Am. Chem. Soc.* **1984**, *106*, 765–784. (b) Weiner, S. J.; Kollman, P. A.; Nguyen, D. T.; Case, D. A. *J. Comput. Chem.* **1986**, *7*, 230–252.

(14) (a) Case, D. A. *J. Biomol. NMR* **1995**, *6*, 341–346. (b) Xu, X.; Case, D. A. *J. Biomol. NMR* **2002**, *21*, 321–333.

(15) Srinivasan, N.; Sowdhamini, R.; Ramakrishnan, C.; Balaram, P. *Int. J. Pept. Protein Res.* **1990**, *36*, 147–155.

(16) Laskowski, R. A.; MacArthur, M. W.; Moss, D. S.; Thornton, J. M. *J. Appl. Crystallogr.* **1993**, *26*, 283–291.

(17) Wang, L.; O’Connell, T.; Tropsha, A.; Hermans, J. *J. Mol. Biol.* **1996**, *262*, 283–293.

(18) Yang, A.-S.; Honig, B. *J. Mol. Biol.* **1995**, *252*, 366–376.

**Chart 1.** Disulfide-Cyclized “bhp” Peptides<sup>a</sup>

CTWEGNKLTC	<b>1</b>	“bhpW”
CT_XEGNKLTC		X3 series <sup>3</sup>
CXWEGNKLTC		X2 series
X = W	<b>2</b>	
F	<b>3</b>	
L	<b>4</b>	
I	<b>5</b>	
V	<b>6</b>	
H	<b>7</b>	
CTWEGNKLXC		X9 series
X = W	<b>8</b>	
F	<b>9</b>	
L	<b>10</b>	
I	<b>11</b>	
V	<b>12</b>	
H	<b>13</b>	
CVWEGNKLHC	<b>14</b>	V2H9 pair (“VH”)
CHWEGNKLVC	<b>15</b>	H2V9 pair (“HV”)
CTWKGNELTC	<b>16</b>	bhpW, KGNE turn
CVWKGNELTC	<b>17</b>	KGNE, V2T9
CTWKGNELVC	<b>18</b>	KGNE, T2V9
CVWKGNELVC	<b>19</b>	KGNE, V2V9
CHXEGNKLVC		HV, X3 series
X = Y	<b>20</b>	
F	<b>21</b>	
L	<b>22</b>	
I	<b>23</b>	
V	<b>24</b>	
A	<b>25</b>	

<sup>a</sup> All peptides were synthesized as C-terminal amides and were acetylated on the N-terminus.

rank order of residue preferences at each of these positions is rather different than what we observed previously for the NHB position 3 (Figure 2a).<sup>3</sup> Significantly, the pattern of stability changes for position 2 is completely different from that of position 9. In contrast, residue preferences are the same for positions 3 and 8.<sup>6</sup> Therefore, in addition to the influence of a cross-strand hydrogen bond between residues 2 and 9, the bhp hairpins exhibit a localized asymmetry that complicates analysis of residue preferences in these sites.

It is possible that the asymmetry in residue preferences at positions 2 and 9 reflects differences in contacts with nearby side chains. We therefore prepared peptides in which a valine residue was paired with a cross-strand histidine instead of a threonine. We also swapped residues 4 and 7, whose side chains are on the same face of the hairpin as residues 2 and 9 (Figure 1b). (In another hairpin model system, “diagonal” interactions between side chains of *non-hydrogen-bonding* residues, placed in proximity by the interstrand twist as are *hydrogen-bonding* residues 4 and 9 here (Figure 1b), have been proposed to influence hairpin stability.<sup>19</sup>) In both cases, the strong stabilizing effect of valine at position 9 remains (Figure 3). It would seem, therefore, that some structural feature other than particular side-chain–side-chain contacts is responsible for this effect.

Tryptophan residues at non-hydrogen-bonding strand positions have been associated with a distinct twist in  $\beta$ -hairpin structures;<sup>3,7</sup> it is possible that this creates a local conformational distortion, influencing residue preferences at adjacent positions. To investigate this, we fixed residues 2 and 9 in the more stabilizing “HV” combination, and then we varied position 3.

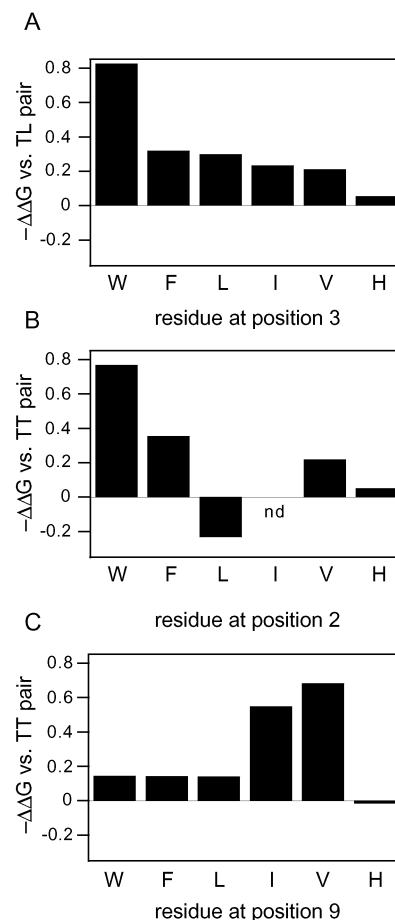


**Figure 2.** Relative stabilities of bhpW analogues. Free-energy changes (293 K) are calculated from the ratio of the cysteine effective concentration ( $C_{\text{eff}}$ ) for each peptide (Supporting Information Table 11) to that of the threonine analogue using the relationship  $-\Delta\Delta G = RT \ln(C_{\text{eff},X}/C_{\text{eff},T})$  and are given in kcal mol<sup>-1</sup>. (The guest site cross-strand partners are leucine or threonine, as noted on the y-axis legends.) (A) Previously reported substitutions at non-hydrogen-bonded strand site 3.<sup>3</sup> (B) Substitutions at position 2 (X2 series 2–7; Chart 1). For the peptide having Ile at position 2 (5), the reduced and oxidized peptides could not be separated by HPLC, preventing the determination of  $C_{\text{eff}}$ . (C) Substitutions at position 9 (X9 series 8–13; Chart 1).

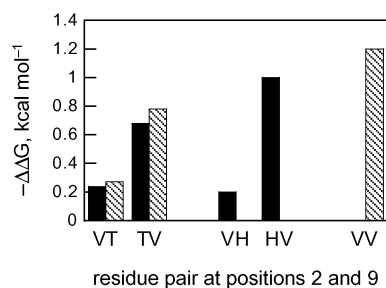


**Figure 3.** Relative stabilities of bhp hairpins with valine at position 2 and 9. Solid bars indicate substitutions in the peptide bhpW (1, 6, 12, 14, 15; Chart 1), while hatched bars correspond to peptides with the altered turn sequence KGNE (16–19; Chart 1). We did not prepare VH or HV variants of the turn-altered peptide and could not measure  $C_{\text{eff}}$  for the VV analogue of bhpW (the reduced peptide aggregated under the conditions of the assay). Free-energy changes (293 K) are calculated from the ratio of peptide  $C_{\text{eff}}$  to that of the appropriate TT analogue (1 or 16;  $-\Delta\Delta G = RT \ln(C_{\text{eff},XX}/C_{\text{eff},TT})$ ).

The relative stabilities of these peptides are compared to those of the analogous T2T9 peptides<sup>3</sup> in Figure 4. The HV peptides are uniformly more stable than their TT counterparts, as

(19) Syud, F. A.; Stanger, H. E.; Gellman, S. H. *J. Am. Chem. Soc.* **2001**, *123*, 8667–8677.

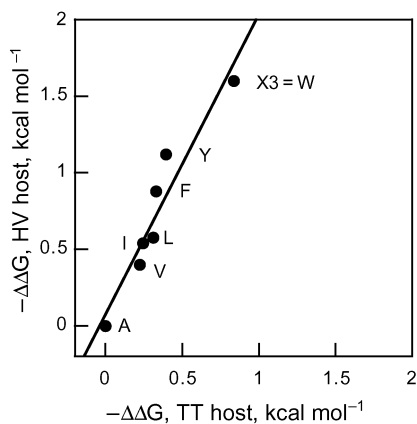


**Figure 4.** Correlation of position 3 substitution free-energy differences for TT bhp analogues (e.g., **1**) and for the HV, X3 series (**15**, **20–25**; Chart 1). The residue substituted at position 3 is indicated, and the slope of the plot is 1.96 ( $R = 0.95$ ). Measurements for the TT bhp series were previously reported in ref 3.  $C_{\text{eff}}$  and  $\Delta\Delta G$  values are listed in Supporting Information Table 11.

indicated by their higher  $C_{\text{eff}}$  values (see Supporting Information). Significantly, the substitution free-energy differences within each series are linearly correlated. This demonstrates that the large stabilization imparted by the valine 9 substitution does not depend on the presence of a particular residue pair at the neighboring non-hydrogen-bonded sites. Interestingly, the slope of the plot is not 1, but instead indicates that the HV host is more sensitive to substitutions at position 3 by a factor of 2. Taken together, the data in Figures 2–4 suggest that the strong, asymmetric stabilization by valine at position 9 is a general property of  $\text{CX}_8\text{C}$  disulfide-constrained hairpins. Indeed, we have previously observed Val9 to be highly stabilizing relative to leucine in an otherwise unrelated  $\text{CX}_8\text{C}$  hairpin.<sup>20</sup>

To assess the effect that the substitutions at the HB site had on hairpin conformation, structures were determined for HV and VH on the basis of  $^1\text{H}$  NMR data (Figure 5). The NMR data for HV are in full agreement with this being a highly structured  $\beta$ -hairpin (Supporting Information Table 1); the  $^1\text{H}$  NMR secondary chemical shifts (the differences between observed and random coil shifts) are much larger than those for bhpW, and  $^3J_{\text{H}\alpha\text{-H}\beta}$  coupling constant values indicate defined side-chain rotamers for three pairs of strand residues (Cys1–Cys10, His2–Val9, Trp3–Leu8; Table 1). In particular, His2 and Val9 can be unambiguously assigned to adopt  $\chi_1$  rotamers of  $+60^\circ$  and  $180^\circ$ , respectively. For peptide VH, the restraints generated from the NMR data clearly define a conformation (Figure 5), but the  $\text{H}^\alpha$  secondary chemical shifts are less extreme than those for HV. Furthermore,  $^3J_{\text{H}\alpha\text{-H}\beta}$  coupling constants indicate motional averaging for the Val2, His9, Trp3, and Leu8 side chains (Table 1; Supporting Information Table 2). All of these features indicate reduced stability for VH as compared to that for HV, consistent with the  $C_{\text{eff}}$  measurements. The relative structural stability of HV and VH does not depend on the presence of histidine; very similar NMR parameters are also observed for peptides in which the histidine is replaced by threonine (Table 1; Supporting Information Tables 3 and 4). That is, TV has well-defined side-chain conformations, whereas VT exhibits conformational averaging at the side-chain level.

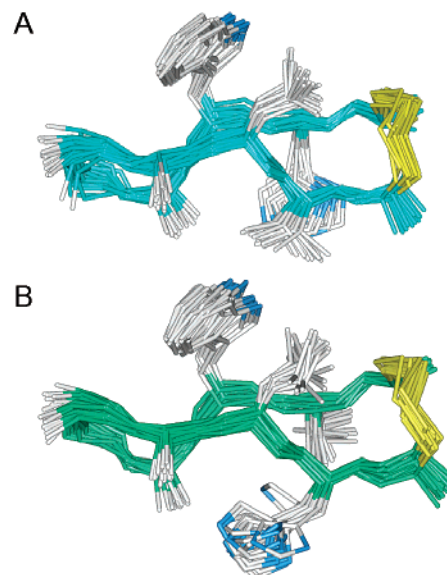


**Figure 5.** NMR structures of bhp peptides HV (**15**) and VH (**14**). The side chains of Cys1 and Cys10 are shown in yellow. For Glu4, Asn6, and Lys7, only the  $\beta$ -carbon of the side chain is shown. (A) Ensemble of 20 structures of HV. The mean rmsd from the mean coordinates is  $0.29 \pm 0.08$  Å. Structures were calculated using 94 NOE distance restraints (19 intraresidue, 25 sequential, 50 medium/long range), 15 dihedral angle restraints (9  $\phi$ , 6  $\chi_1$ ), and 37  $^1\text{H}$  chemical shift restraints. (B) NMR structures of VH. For the 20 lowest energy structures, the mean backbone rmsd from the mean coordinates is  $0.29 \pm 0.05$  Å. Structures were calculated using 74 NOE distance restraints (12 intraresidue, 23 sequential, 39 medium/long range), 11 dihedral angle restraints (9  $\phi$ , 2  $\chi_1$ ), and 8  $^1\text{H}$  chemical shift restraints. Coordinates for the HV and VH ensembles, as well as for the TT analogue bhpW (**1**),<sup>3</sup> have been deposited in the RCSB Protein Data Bank (<http://www.pdb.org>) under accession codes 1N0C, 1N0D, and 1N09, respectively.

The structures determined for HV and VH are quite similar at the backbone level (rms difference of  $0.37$  Å between the mean structures): both peptides adopt a type II' turn and have a considerable right-handed twist of the strands, as was seen previously for bhpW.<sup>3</sup> Calculation of the interstrand twist angle indicates that for the cyclized hairpins, the twist is not uniform (Supporting Information Table 9), with less twisting adjacent to the disulfide ( $\Theta < 20^\circ$  between the Cys1, Cys10 pair and the 2, 9 pair) and more twisting before and after the NHB pair Trp3, Leu8 ( $\Theta \approx 30^\circ$ ). Because these measurements involve atoms from both strands, the degree of twist present in each individual strand is not apparent from  $\Theta$ . Alternatively, the sum of  $\psi$  from one residue and  $\phi$  from the succeeding residue ( $\psi_i + \phi_{i+1}$ ) gives an indication of the twist between consecutive  $\alpha$ -carbons in the same strand, with nontwisted strands having a value of zero, and strands of right-handed twist having a positive value. The twist data for the HV and VH ensembles are compared to the data of bhpW in Figure 6 (and listed in Supporting Information Table 9). These data clearly indicate that the majority of the twist contributing to the large interstrand  $\Theta$  values occurs on the N-terminal side of the NHB hydrophobic residues ( $45\text{--}65^\circ$  between His/Val/Thr2 and Trp3, and between Lys7 and Leu8, as compared to  $<20^\circ$  between Trp3 and Glu4 and between Leu8 and Val/His/Thr9). Although the ranges of  $\psi_i + \phi_{i+1}$  within the three ensembles overlap, the data in Figure 6 indicate that as compared to VH, HV has a slightly more pronounced twist preceding the NHB sites and a less pronounced twist around Cys1; assuming a normal distribution of dihedral angles within each ensemble, an independent samples t-test

(20) Skelton, N. J.; Russell, S.; de Sauvage, F.; Cochran, A. G. *J. Mol. Biol.* **2002**, *316*, 1111–1125.

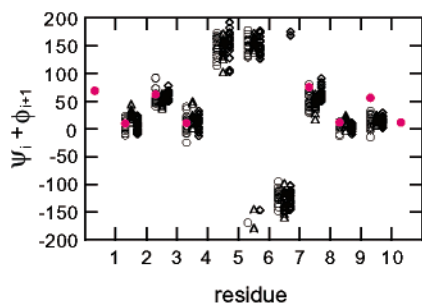


**Figure 6.** Position-specific strand twists ( $\psi_i + \phi_{i+1}$ ) for the 20 structures in the ensembles determined for bhpW (1; left  $\circ$ ), VH (14; center  $\Delta$ ), and HV (15; right  $\diamond$ ). Pink filled circles indicate the average values for the more uniformly coiled strand residues of trpzip47 (see below) aligned with the corresponding residues of the shorter bhp strands.

indicates that the mean  $\psi_i + \phi_{i+1}$  for HV and VH are different for residues 1–2, 2–3, and 7–8 with a p-value of less than 0.01. This suggests that swapping the location of His and Val side chains does have a subtle influence on backbone geometry.

The main difference between the HV and VH ensembles is the degree of side-chain order. Although Cys1, Trp3, Leu8, and Cys10 adopt the same  $\chi_1$  in HV and VH ( $-60^\circ$  for Cys1, Trp3, and Cys10;  $180^\circ$  for Leu8), the magnitudes of the  $^3J_{\text{H}\alpha\text{-H}\beta}$  are less extreme in the latter, suggesting that the side chains of VH are transiently sampling alternate conformations. More importantly, in HV the  $\chi_1$  rotamers of His2 and Val9 are fixed ( $+60^\circ$  and  $180^\circ$ , respectively) bringing these two side chains into van der Waals contact above the cross-strand hydrogen bonds. Because of the twisting of the strands, the  $\gamma_2$  methyl group of Val9 is also brought into van der Waals contact with the side-chain methylene groups of both Glu4 and Lys7. However, in VH, Val2 populates both the  $-60^\circ$  and the  $180^\circ$  rotamer wells, and most of the structures in the ensemble have a  $\chi_1$  of  $-60^\circ$  for His9, orienting the side chain in the direction of the turn. Moreover, the twisting of the strands directs the Val2 side chain toward the termini of the peptide. Thus, there is little or no contact between these side chains, and the backbone hydrogen bond between these residues is more exposed to solvent.

To assess whether the asymmetric stabilization seen for the HV peptide was related to differences in interstrand twist imposed by the disulfide bond, peptides HV and VH were examined by NMR after reduction (Supporting Information Tables 5 and 6). Surprisingly, reduced HV has observable residual structure: four  $^3J_{\text{H}^{\text{N}}\text{-H}^\alpha}$  coupling constants exceed 8 Hz, Leu8 methyl chemical shifts are 0.41 and 0.33 ppm upfield as compared to those of random coil, and three backbone cross-strand NOEs are observed (Cys1  $\text{H}^\alpha$  to Cys10  $\text{H}^\alpha$ , His2  $\text{H}^{\text{N}}$  to Val9  $\text{H}^{\text{N}}$ , and Glu4  $\text{H}^{\text{N}}$  to Lys7  $\text{H}^{\text{N}}$ ). In contrast, there are no indications that reduced VH has a preferred conformation. Presumably, Val9 can adopt a similar conformation in the reduced peptide as it does in the oxidized form, while the strong right-handed twist of the strands preceding position 3 (see above) would not allow the Val2 side chain of either form to interact with the C-terminal strand.

To examine this further, we made analogous substitutions in a more structurally stable uncyclized  $\beta$ -hairpin peptide. Tryptophan zippers (trpzips) are short peptides that adopt unusually stable hairpin conformations.<sup>7</sup> The  $\beta$ -strands of trpzips consist of the core sequence WTW paired with WTW on the opposite strand; the tryptophan residues occupy the non-hydrogen-bonded strand sites. Because of their unusual stability ( $\sim 1\text{--}2 \text{ kcal mol}^{-1}$

**Chart 2.** Tryptophan Zipper “Trpzip” Peptides<sup>7,a</sup>

GEW <b>T</b> WDDATK <b>T</b> W <b>T</b> WTE	trpzip4
GEW <b>V</b> WDDATK <b>T</b> W <b>H</b> WTE	trpzip7
GEW <b>H</b> WDDATK <b>T</b> W <b>V</b> WTE	trpzip8
GEW <b>V</b> WDDATK <b>T</b> W <b>V</b> WTE	trpzip9

<sup>a</sup> All peptides were synthesized as C-terminal amides. Trpzip4 is described in ref 7.

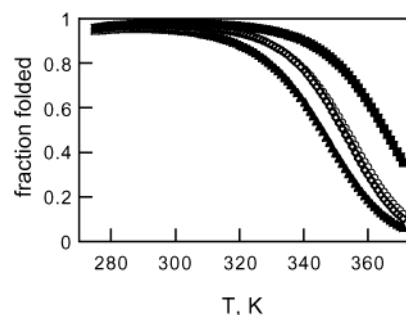


**Figure 7.** Thermal denaturation curves of “trpzip” variants (Chart 2). Trpzip4 data (TT pair,  $T_m = 343 \text{ K}$ ) are shown as  $\blacktriangle$  (taken from ref 7), trpzip7 (VH pair,  $T_m = 352 \text{ K}$ ) as  $\diamond$ , trpzip8 (HV pair,  $T_m = 353 \text{ K}$ ) as  $\circ$ , and trpzip9 (VV pair,  $T_m = 365 \text{ K}$ ) as  $\blacksquare$ . Thermal denaturation data were acquired and analyzed as previously described.<sup>7</sup>

at room temperature) and the unique spectroscopic properties conferred by the two tryptophan–tryptophan pairs, it is possible to monitor the folding of the trpzips by circular dichroism.<sup>7</sup> The trpzip peptides are monomeric and undergo reversible thermal denaturation, allowing the determination of thermodynamic folding parameters from the melting curves. The most stable of the reported trpzips is trpzip4 (Chart 2) which was based on a partially folded peptide taken from the C-terminal hairpin of the IgG-binding protein GB1.<sup>21</sup> We therefore introduced histidine and valine substitutions into trpzip4 (Chart 2).

Trpzips 7 and 8 were analyzed by NMR spectroscopy (Supporting Information Tables 7 and 8). In both peptides,  $^1\text{H}$  chemical shifts and coupling constants are generally similar to those of trpzip4 and are characteristic of well-folded hairpins.<sup>7</sup> However, in both peptides, the intermediate values for the  $^3J_{\text{H}\alpha\text{-H}\beta}$  coupling constants of histidine and valine indicate that these side chains do not adopt specific  $\chi_1$  rotamers (Table 1). This is in contrast to the equivalent substitutions in the bhpW background, where very well-defined side-chain orientations are present in the oxidized HV analogue.

Thermal denaturation curves of trpzips 7–9 are compared to that of trpzip4 in Figure 7. Both HV and VH pairs are stabilizing as compared to the original TT pair, and VV is the most stabilizing pair tested. However, reversing the positions of histidine and valine does not significantly affect the stability of the hairpin ( $\Delta G_{\text{unfold}, 293 \text{ K}} = 1.78, 2.04, 1.99, \text{ and } 2.21 \text{ kcal mol}^{-1}$  for trpzips 4, 7, 8, and 9, respectively). Instead, each histidine–valine pair is  $\sim 0.2 \text{ kcal mol}^{-1}$  more stabilizing than TT and  $0.2 \text{ kcal mol}^{-1}$  less stabilizing than VV. This is very close to the stability changes seen for V2 substitutions in the cyclic bhp peptides (Figure 3). There is no large stability change in the trpzips analogous to that seen for V9 bhp peptides.

## Discussion

We have found that disulfide-cyclized  $\beta$ -hairpins can be markedly stabilized by a valine residue immediately preceding the C-terminal cysteine. Isoleucine appears to be nearly as

(21) Blanco, F. J.; Rivas, G.; Serrano, L. *Nat. Struct. Biol.* **1994**, *1*, 584–590.

stabilizing, while the other  $\beta$ -branched amino acid threonine and aromatic residues are not particularly stabilizing. This pattern of residue preferences differs strongly from reported  $\beta$ -propensity scales and, significantly, from that of the analogous site (position 2) on the other strand of the hairpin. We attribute this effect to a favorable conformational relationship between Val9 and Cys10; when valine substitutions are introduced into the equivalent sites of a linear  $\beta$ -hairpin with a more regular backbone geometry (trpzip series), the large, asymmetric contribution from the more C-terminal substitution is absent. Instead, a more modest increase in stability is seen for both valine-substituted peptides.

Evidence for these conformational relationships may be seen in a detailed examination of the peptide structures. In the case of the more energetically symmetric trpzip scaffold, there is a high degree of backbone twist preceding all four NHB tryptophan residues, resulting in a regular coiling of the strands (Figure 6). In contrast, the twisting of the CX<sub>8</sub>C scaffold is not uniform. A high degree of twist precedes only the hydrophobic NHB sites 3 and 8, with much less twist preceding the cysteine residues. The occurrence of right-handed twist in antiparallel  $\beta$  structures has been attributed to intrastrand side-chain-to-backbone van der Waals contacts,<sup>22</sup> cross-strand nonpolar side-chain interactions,<sup>18</sup> or backbone electrostatic interactions.<sup>17,23</sup> These computational studies demonstrate that a right-handed twist is energetically favorable and that for two-stranded interactions, a pronounced twist (the maximum twist that still permits good geometry for the cross-strand hydrogen bonds) is most stable.<sup>17,18</sup> Thus, the twist observed at the NHB hydrophobic sites of the CX<sub>8</sub>C peptides and in the tryptophan zipper peptides allows optimal interactions between the two strands.

However, an interstrand disulfide has different backbone geometric requirements. Several groups have described the formation of cystine bonds between adjacent antiparallel strands in proteins;<sup>8,24</sup> such disulfides are quite rare and are restricted to NHB cysteine pairs. Furthermore, the cross-strand disulfide always adopts a particular geometry that is distinct from the canonical disulfide conformations described by Richardson.<sup>25</sup> (For this reason, early designs of disulfide-cyclized hairpins often included one or more D-cysteine residues that were thought to be more compatible with antiparallel  $\beta$  geometry.<sup>26</sup>) A survey of the disulfide-containing structures listed in Gunasekaran et al.<sup>8a</sup> indicates that, in general,  $\Theta$  on either side of the disulfide is  $<20^\circ$ . Thus, the disulfide backbone geometry is suboptimal for strand–strand interactions, and the conformation observed in our CX<sub>8</sub>C peptides is a compromise between stable strand pairing and a stable disulfide conformation. Interestingly, the observation of residual structure in reduced HV, but not in reduced VH, suggests that the packing of a reduced cysteine NHB pair may be insufficient to impose a fully twisted conformation, at least when placed at the termini of a marginally structured hairpin. A less twisted conformation is, however,

more typical of  $\beta$ -sheets in proteins,<sup>18</sup> which seldom consist of isolated two-stranded structures.

It is possible that the greater structural stability of the HV hairpin is determined by local sequence differences (other than the disulfide) that do not exist in the analogous trpzip peptides. To address this question, we compared free-energy differences for substitutions at position 3 in two different backgrounds, the original T2T9 bhp scaffold and the more stable H2V9 variant (Figure 4). We found a very strong linear correlation, demonstrating that the H2V9 substitution does not alter the energetic properties of the 3,8-pair and, likewise, that the W3L8 pair present in “HV” is not required for its unusual stability. Instead, these data suggest that the stabilizing effect of valine in these peptides is general for the CX<sub>8</sub>C hairpin fold and that the effect is confined to the favorable conformational interaction between Val9 and Cys10 discussed above. The low degree of interstrand twist preceding the disulfide orients the Val9 side chain toward the opposite strand; the Val9 side chain may shield the 2,9-hydrogen bonds from solvent, thereby stabilizing the structure.

An especially interesting feature of the correlation shown in Figure 4 is the slope of 2. This shows not only that the peptides have the same relative residue preferences at position 3 but, in addition, that the free-energy differences are amplified in the more stable “HV” background. Previously, we observed a similar amplification of position 3 free-energy changes in peptides with the stabilizing L8W substitution<sup>6</sup> (and, more recently, an analogous correlation for mutants of the model  $\beta$ -sheet protein GB1<sup>27</sup>). These data demonstrate that nonadditive contributions from particular pairwise combinations of residues do not necessarily imply that the side chains interact with each other; indeed, the side chains at positions 3 and at 2 or 9 are on opposite faces of the hairpin and cannot contact each other in the folded peptide. In our hairpins, stabilizing strand substitutions uniformly enhance the contributions from residues at other strand sites, consistent with the idea of a “funnel-like” folding free-energy surface.<sup>28</sup> Previously, it has been observed that  $\beta$ -hairpins undergo cooperative thermal unfolding transitions,<sup>7,29</sup> and in many published studies of designed three-stranded sheets, it appears that association of a third strand with a hairpin is cooperative.<sup>30</sup> However, the data we present here would seem to go beyond this, indicating that strand–strand association is itself cooperative, even at the level of one three-residue strand associating with another. Possibly, stabilizing substitutions synergize through enhanced desolvation of cross-strand hydrogen bonds. In contrast, we have observed that  $\beta$ -turns and strands contribute in a strictly additive way to the stability of the bhp hairpins; free energies are correlated for substitutions in peptides with different turn sequences (as in Figure 4) but with slopes close to 1.<sup>3</sup>

(22) Chou, K.-C.; Scheraga, H. A. *Proc. Natl. Acad. Sci. U.S.A.* **1982**, *79*, 7047–7051.

(23) Maccallum, P. H.; Poet, R.; Milner-White, E. J. *J. Mol. Biol.* **1995**, *248*, 374–384.

(24) Wouters, M. A.; Curmi, P. M. G. *Proteins* **1995**, *22*, 119–131.

(25) Richardson, J. S. *Adv. Protein Chem.* **1981**, *34*, 167–330.

(26) (a) Sieber, V.; Moe, G. R. *Biochemistry* **1996**, *35*, 181–188. (b) McDonnell, J. M.; Beavil, A. J.; Mackay, G. A.; Jameson, B. A.; Korngold, R.; Gould, H. J.; Sutton, B. J. *Nat. Struct. Biol.* **1996**, *3*, 419–426. (c) McDonnell, J. M.; Fushman, D.; Cahill, S. M.; Sutton, B. J.; Cowburn, D. *J. Am. Chem. Soc.* **1997**, *119*, 5321–5328.

(27) Distefano, M. D.; Zhong, A.; Cochran, A. G. *J. Mol. Biol.* **2002**, *322*, 179–188.

(28) Dobson, C. M.; Sali, A.; Karplus, M. *Angew. Chem., Int. Ed.* **1998**, *37*, 868–893.

(29) (a) Muñoz, V.; Thompson, P. A.; Hofrichter, J.; Eaton, W. A. *Nature* **1997**, *390*, 196–199. (b) Maynard, A. J.; Sharman, G. J.; Searle, M. S. *J. Am. Chem. Soc.* **1998**, *120*, 1996–2007. (c) Honda, S.; Kobayashi, N.; Munekata, E. *J. Mol. Biol.* **2000**, *295*, 269–278. (d) Espinosa, J. F.; Gellman, S. H. *Angew. Chem., Int. Ed.* **2000**, *39*, 2330–2333.

(30) (a) Sharman, G. J.; Searle, M. S. *J. Am. Chem. Soc.* **1998**, *120*, 5291–5300. (b) Schenck, H. L.; Gellman, S. H. *J. Am. Chem. Soc.* **1998**, *120*, 4869–4870. (c) Griffiths-Jones, S. R.; Searle, M. S. *J. Am. Chem. Soc.* **2000**, *122*, 8350–8356. (d) López de la Paz, M.; Lacroix, E.; Ramírez-Alvarado, M.; Serrano, L. *J. Mol. Biol.* **2001**, *312*, 229–246.

Interestingly, the cooperativity we observe in strand–strand association is reminiscent of an effect observed in studies of helical peptides. It has been found that helical propensities measured in guest sites of proteins correlate with those measured in the corresponding excised peptides and also with those measured in alanine-stabilized helices.<sup>31</sup> However, a curious (and as yet unexplained) difference is the much larger range of free-energy differences observed in the multiply alanine-substituted peptide series.<sup>31,32</sup> It is notable that these alanine helices are generally much more helical than peptides of more mixed composition, so perhaps this too represents cooperative folding at a very local level.

Finally, the stabilizing motifs we have defined for the bhp hairpins might have been predicted from examination of similar hairpins selected from phage-displayed peptide libraries. Representative examples from the CX<sub>8</sub>C class are shown in Chart 3. In addition to a Gly-Pro type-I turn sequence (not varied in these libraries), the common feature selected is the Trp-Val sequence immediately preceding the second cysteine. From the data we report here and from our earlier studies,<sup>6</sup> this is the most stabilizing (and likely optimal) residue combination at these two positions, suggesting that the phage binding selection is also a strong selection for structural stability. It is interesting that more variability is seen at position 3, where a Trp residue

**Chart 3.** “WVC” Peptide Ligands Selected from Phage-Displayed Libraries<sup>a</sup>

GGTYS	CHFGP	L T	WVCKPQGG	EMP1
Ac-NLPR	CTEGPWG	WVCM		IGE06
GERWC	FDGP	RAWVCGWEI		v106

<sup>a</sup> Peptide EMP1 binds as a dimer of  $\beta$ -hairpins to two monomers of the erythropoietin receptor (EpoR), mimicking the function of the cytokine Epo.<sup>20,33</sup> Peptide IGE06 forms a stable  $\beta$ -hairpin in solution that blocks association of IgE with the high-affinity IgE receptor.<sup>34</sup> Peptide v106 blocks the binding of the vascular endothelial growth factor (VEGF) to its receptor KDR and appears to bind as a  $\beta$ -hairpin.<sup>35</sup>

would also be highly stabilizing.<sup>3,6</sup> Perhaps the selected Trp is more useful as part of a “WVC” strand that may nucleate the hairpin structure, leaving other residues (including the other strand) free to form productive binding contacts. A continuous motif may also be especially effective in destabilizing alternative helical folds.<sup>20</sup>

Our original purpose in investigating the bhp hairpins was to develop stable, structurally biased scaffolds for phage display. For  $\beta$ -turn display, the combination of a Trp residue at position 3 or 8<sup>6</sup> and the very stabilizing His-Val 2,9-pair we report here would appear especially useful. As compared to the least stable combinations in which definite hairpin structure is detectable,<sup>3</sup> these substitutions stabilize the fold by more than 1.5 kcal mol<sup>-1</sup>. Inclusion of the optimal W3–W8 pair should increase stability further, expanding the range of  $\beta$ -turns that might be structured.<sup>3</sup> Our data further suggest that libraries with fixed CX<sub>n</sub>WVC motifs might also be useful in generating structured hairpin ligands.

**Supporting Information Available:** Tables S1–S11 detailing NMR assignments and coupling constants for peptides HV, VH, TV, VT, reduced HV, reduced VH, trpzip7, and trpzip8; calculated strand twist for peptides bhpW, VH, HV, and trpzip4; details of restraints and structural statistics for bhpW, VH, and HV; and  $C_{\text{eff}}$  values for the peptides in Chart 1 (PDF). This material is available free of charge via the Internet at <http://pubs.acs.org>.

JA028075L

(31) Myers, J. K.; Pace, C. N.; Scholtz, J. M. *Proc. Natl. Acad. Sci. U.S.A.* **1997**, *94*, 2833–2837.

(32) Baldwin, R. L.; Rose, G. D. *Trends Biochem. Sci.* **1999**, *24*, 26–33.

(33) (a) Wrighton, N. C.; Farrell, F. X.; Chang, R.; Kashyap, A. K.; Barbone, F. P.; Mulcahy, L. S.; Johnson, D. L.; Barrett, R. W.; Jolliffe, L. K.; Dower, W. J. *Science* **1996**, *273*, 458–463. (b) Livnah, O.; Stura, E. A.; Johnson, D. L.; Middleton, S. A.; Mulcahy, L. S.; Wrighton, N. C.; Dower, W. J.; Jolliffe, L. K.; Wilson, I. A. *Science* **1996**, *273*, 464–471. (c) Johnson, D. L.; Farrell, F. X.; Barbone, F. P.; McMahon, F. J.; Tullai, J.; Hoey, K.; Livnah, O.; Wrighton, N. C.; Middleton, S. A.; Loughney, D. A.; Stura, E. A.; Dower, W. J.; Mulcahy, L. S.; Wilson, I. A.; Jolliffe, L. K. *Biochemistry* **1998**, *37*, 3699–3710. (d) Livnah, O.; Johnson, D. L.; Stura, E. A.; Farrell, F. X.; Barbone, F. P.; You, Y.; Liu, K. D.; Goldsmith, M. A.; He, W.; Krause, C. D.; Petska, S.; Jolliffe, L. K.; Wilson, I. A. *Nat. Struct. Biol.* **1998**, *5*, 993–1004.

(34) Nakamura, G. R.; Starovasnik, M. A.; Reynolds, M. E.; Lowman, H. B. *Biochemistry* **2001**, *40*, 9828–9835.

(35) (a) Fairbrother, W. J.; Christinger, H. W.; Cochran, A. G.; Fuh, G.; Keenan, C. J.; Quan, C.; Tom, J. Y. K.; Wells, J. A.; Cuningham, B. C. *Biochemistry* **1998**, *37*, 17754–17764. (b) Pan, B.; Li, B.; Russell, S. J.; Tom, J. Y. K.; Cochran, A. G.; Fairbrother, W. J. *J. Mol. Biol.* **2002**, *316*, 769–787.